

Fractal Sandstone Pores: Implications for Conductivity and Pore Formation

A. J. Katz and A. H. Thompson

Exxon Production Research Company, Houston, Texas 77001

(Received 4 June 1984)

We use scanning electron microscopy and optical data to show that the pore spaces of several sandstones are fractal geometries and we use the fractal statistics to predict the correct porosity. Steady-state crystal growth during rock formation is a plausible cause of the self-similar geometry. The fractal-dimension values and a systematic analysis of rock conductivity data both mediate against percolation models as suitable models of rock pore-space geometry.

PACS numbers: 91.60.Pn, 05.60.+w

We present experimental evidence indicating that the pore spaces of a set of sandstone samples are fractals¹ and are self-similar over 3 to 4 orders of magnitude in length extending from 10 Å to over 100 μm. The measured values of the fractal dimensions are greater than those expected for a three-dimensional, random mixture near the percolation threshold,² which suggests that percolation theory does not describe the pore-space geometry. The fractal dimension varies from sample to sample with extreme values of 2.57 to 2.87. This range of values suggests that the pore formation processes do not fall within a single universality class.

The density-density correlation function of the pore space is constant over length scales greater than a characteristic length l_2 , which is approximately the size of sand grains in a sandstone (typically 100 μm across). For length scales $l > l_2$, we expect the transport coefficients to be constant and characteristic of the macroscopic properties of the rock. At length scales $l_1 < l < l_2$, we show that the pore-space-rock interface is a self-similar manifold with a well-defined fractal dimension, D , and a lower limit of self-similarity, l_1 .

We further argue that the pore volume is a fractal with the same fractal dimension as the pore-rock interface. This conclusion is supported by correctly predicting the porosity from the fractal parameters and by directly showing that the fractal dimension measured by autocorrelation of pores on thin sections agrees with that measured on fracture surfaces.

We also show that self-similar pore-space geometries can arise naturally from crystal growth in pore spaces under quasi-steady-state conditions and that the resulting fractal dimensions can assume a continuous range of values that depend on *chemical* kinetic parameters. Self-similarity in rock pore spaces leads naturally to an explanation of Archie's law for the conductivity. We find that the literature conductivity data cannot be used to draw any conclusions regarding the presence (or absence) of a percolation threshold.

Measurements of the electrical conductivity of rocks play an important role in oil and mineral exploration and production. For many sandstones saturated with

saline solution, the electrical conductivity follows the empirical Archie formula,³ $\sigma = \sigma_w \phi^m$, where σ is the rock conductivity, σ_w is the conductivity of the pore fluid, ϕ is the porosity, and m is an exponent, which is traditionally defined by log-log plots of σ vs ϕ . Archie's law depends on the geometry of the pore space, but there exists no detailed understanding of this relation.

Previous attempts to understand the electrical conductivity of rocks fall in the realm of either effective-medium theory or percolation theory. Differential effective-medium models⁴ yield expressions for the conductivity that are power laws in porosity, but these expressions apply to both self-similar geometries (Ref. 4 suggests that rock-pore spaces may be self-similar) and other arrangements such as sphere packs. Recent experiments on sintered-glass sphere packs⁵ show that the measured conductivity is not a power law in porosity. These experiments emphasize the inadequacy of the effective-medium treatment and of sphere-pack models for rocks.

We measure fractal parameters on rock fracture surfaces utilizing the secondary-electron emission from a scanning electron microscope (SEM). The structures we examine lie below the fracture plane so that *the measured parameters do not depend on the fracture geometry*. The SEM measurement defines the fractal dimension of a one-dimensional *section* of the pore-rock interface. At each magnification the structure detected by the SEM beam along a linear trace is limited by the microscope resolution; for an isotropic fractal, this resolution limits the depth of field. The SEM depth of field decreases at increasing magnification such that it is always smaller than the depth of the rock interface. There is a one-to-one correspondence between the secondary-electron-intensity extrema and the edges that intersect the line defined by the SEM trace.⁶ The SEM measurement, therefore, provides a count of the number of edge intersections in a one-dimensional section of the interface as a function of magnification. We call the protrusions into the pore space that define these edges geometric features. A log-log plot of the number of features counted at a particular magnification versus the length scale gives

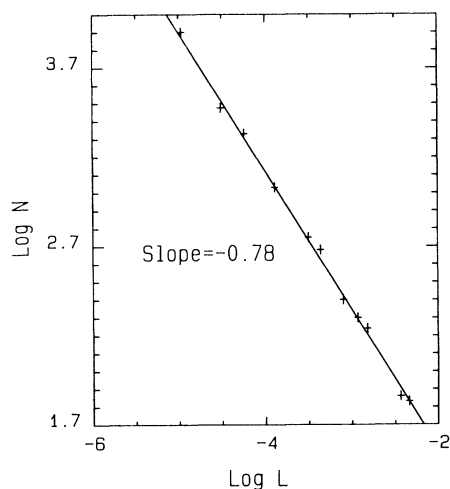


FIG. 1. A log-log plot of the number of geometric features of size L per unit length vs the size L (in centimeters) for Coconino sandstone.

rise to a straight line with slope $2-D$ for a one-dimensional section of an interface with fractal dimension D ($2 < D < 3$). Systematic deviations from the power-law form define the length scales l_1 and l_2 .

Figure 1 is a log-log plot of the number of features of size L per unit length resolved at a given magnification versus the length scale (L) for Coconino sandstone, a sandstone originating in Arizona. At short-length extremes, the data are limited by the microscope resolution of 100 \AA . At the long-length extremes, we used optical-microscope data to find that the linearity on the log-log plot stops at $98 \mu\text{m}$. The fractal dimension D is given by the slope $S = 2 - D$ of Fig. 1. For Coconino sandstone $D = 2.78$.

Our assumption that the sandstone pore space has the fractal properties of the interface implies a simple relationship¹ between the fractal dimension and the porosity of the rock. In a volume element of size l_2 ,

the "volume" of the pore-filling surface is given in units of l_1 by $A(l_2/l_1)^D$, where l_1 is the lower limit of the self-similar region, l_2 is the upper limit, and A is a constant of order one. Hence, the porosity, ϕ , is simply

$$\phi = A(l_1/l_2)^{3-D}. \quad (1)$$

For all the sandstones we consider, we take $A = 1$ and assume that l_1 is a constant on the order of 20 \AA , the minimum size of a crystal nucleus in the pore space. By use of Eq. (1), with $l_2 = 98 \mu\text{m}$ (from optical autocorrelation data), we find that the calculated porosity of Coconino sandstone is 10%, in good agreement with our measured values of 10.8% to 12.5% in various samples.

The analysis of the fractal dimensionality and calculation of the porosity were applied to four other sandstones. The results are shown in Table I. The porosities in Table I were measured with use of Boyle's law methods. The uncertainties in the values of D (on the order of ± 0.02) dominate the uncertainties in the calculated porosity values. Successful prediction of the porosities from the fractal parameters verifies the assumption that the pore surface and volume are fractals with the same fractal dimension.

The conclusion that the pore volume and pore surface have the same fractal dimension is directly supported by pore-pore density autocorrelation measurements on thin sections as shown in Fig. 2. There we compare the autocorrelation function optically measured on SEM images of polished thin sections with the slope of the geometric-feature count from a fracture surface on the same rock. For a fractal pore space we would expect this autocorrelation function to be proportional to L^{D-3} where L is the lag. At short lags the autocorrelation function asymptotically approaches the slope given by the feature count. At large lag the autocorrelation deviates from the power-law slope as neighboring uncorrelated pores are sampled. At the longest lags the homogeneous limit is reached where

TABLE I. Results of SEM measurements on various sandstones.

Sample	Fractal dimension	l_2 (μm)	Porosity (%)	
			Calculated	Measured
Tight gas sand #965	2.57	2.5	4.7	5.3-5.6
Tight gas sand #466	2.68	6	7.6	6.9-7.6
Coconino	2.78	98	10	11-12.5
Navajo	2.81	50	15	16.4
St. Peter's	2.87	50	27	24-28

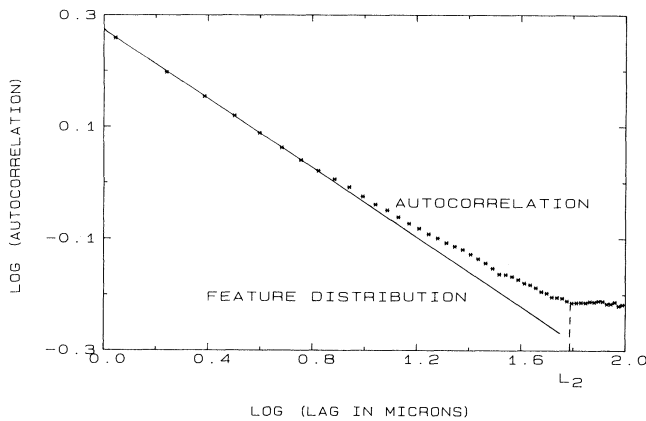


FIG. 2. A log-log plot of the pore-pore density autocorrelation function taken on a quartz cemented sandstone from eastern Utah. The slope of the straight line was taken from the feature-size distribution collected on a fracture surface as in Fig. 1. The autocorrelation data were taken by optical measurements on SEM images of polished-rock thin sections. The units of autocorrelation are arbitrary.

the variance is zero. The length l_2 is defined by the lag at which the autocorrelation is constant. The agreement between the autocorrelation function and the feature count directly shows that the pore-space volume is a fractal and that it has the same fractal dimension as the interface.

The fractal structure of the pore space also suggests that dynamics within the pore space should scale with the length parameter l . Recent papers find that a random walker on a fractal geometry diffuses anomalously.^{2,7-10} From the Einstein relation, we expect the conductivity of a rock sample, which is self-similar for length scales $l_1 < l < l_2$ and homogeneous for length scales $l > l_2$, to be^{2,8-11}

$$\sigma = \sigma_w \phi (l_1/l_2)^{2(D-D_f)/D_f} = \sigma_w \phi^n, \quad (2)$$

where the second equality follows from Eq. (1) and $n = [D_f + D(2 - D_f)] / (3 - D)D_f$. Here σ_w is the ionic conductivity of the fluid filling the pore space and D_f is the spectral dimension. Equation (2) is consistent with the form of Archie's law.

We next present a simple nucleation and growth model that can account for a power-law distribution of feature sizes and is consistent with general constraints governing rock formation. We emphasize that the mineral growth that gives rise to features inside the pore space is very different from dendritic growth. Sandstone formation involves burial of the sand grains, compaction, and then alteration of the pore structure by the flow of fluids through the pore space. Such alteration involves crystal growth and nucleation on the pore surface. The rate-limiting steps for both crystal nucleation and growth of established crystals is

the rate of addition of species to growth sites on the pore surfaces. Diffusion and fluid transport from the pore volume should be rapid by comparison. The number of growth sites is not limiting. We formulate the competing processes of crystal growth and crystal nucleation in terms of two kinetic equations:

$$dR/dt = kc^n, \quad (3)$$

$$dN/dt = k_1 c^p. \quad (4)$$

The first equation describes the growth of a crystal of size R . The second equation describes the heterogeneous nucleation of new crystals on a patch of surface of unit linear dimension. Here c is the concentration of surface molecules and k and k_1 are equilibrium constants. We expect that $n = 1$ since growth involves the addition of a single molecule to a growth site and $p > 1$ since nucleation requires the coincidence of two or more molecules at a nucleation site.¹²

The concentration, c , is a slowly varying function of time over an interval T that is long compared to a crystal growth time but short relative to geologic time. In a time interval T we take c to be constant and solve Eqs. (3) and (4). The ultimate crystal size is limited by nucleation of new crystals on the rock surface so that $R \propto (dR/dt)/(dN/dt)$. The total number of nuclei of size R formed on a surface patch of unit linear dimension in time T is $N(R) = (dN/dt)T$. Over times large compared to T , c increases with time as the pore space fills and as fluid-flow rates decrease. (Note that this time-dependent c is an essential difference between this model and many others involving nucleation and growth.) Since c increases and $p > 1$, the equations for R and $N(R)$ indicate that R decreases with time and $N(R)$ increases; i.e., the number of small crystals increases in time. Combination of the expressions for R and $N(R)$ yields

$$N(R) \propto R^{-p/(p-1)}. \quad (5)$$

Classical nucleation theory requires that $p < 2$ so that $2 \leq p/(p-1)$. Moreover, the imposition that the volume of the particles formed does not exceed the available volume requires that $2 \leq p/(p-1) \leq 3$.

This model provides one possible deterministic model for fractal crystal growth in rocks and is a *mechanism capable of producing fractal pore spaces with a continuous range of dimensionalities*. It also supports our empirical observation that l_1 is of order 20 Å, the size of a crystal nucleus, and limits the fractal dimension to lie between 2 and 3.

Several authors have used the apparent lack of a percolation threshold in sedimentary rocks^{4,5} as a significant clue toward understanding the transport properties. We find, however, that Archie's law can follow directly from the self-similar nature of a specific pore geometry for even the lowest porosities. The Archie's-law form of the conductivity with a well-

defined exponent is predictable only for a particular geometry. In general, each rock-pore geometry will yield an exponent different from all other rocks. The conductivity exponent must then be determined on a rock-by-rock basis since neither D nor D_f takes on a universal value for all sandstones. When Archie's law is applied to literature sandstone data one sample at a time, we find that $1.5 < m < 2.5$ in contrast to the literature values, which range from 0.5 to 5. The practice of representing conductivity data by a power law with zero percolation threshold then makes no sense: We cannot draw conclusions about the transport properties of one rock from those of another with a different pore geometry.

We thank C. E. Krohn for use of her data before publication and S. C. Eno for assistance with the autocorrelation measurement.

¹B. B. Mandelbrot, *The Fractal Geometry of Nature* (Free-

man, San Francisco, 1982).

²S. Alexander and R. Orbach, *J. Phys. (Paris), Lett.* **43**, L625 (1982).

³G. E. Archie, *Bull. Am. Assoc. Pet. Geol.* **36**, 278 (1952).

⁴P. N. Sen, C. Scala, and M. H. Cohen, *Geophysics* **46**, 781 (1981).

⁵D. L. Johnson, T. J. Plona, C. Scala, F. Pasierb, and H. Kojima, *Phys. Rev. Lett.* **49**, 1840 (1982); D. H. Johnson, *Bull. Am. Phys. Soc.* **29**, 333 (1984).

⁶J. L. Goldstein, *Practical Scanning Electron Microscopy*, edited by J. I. Goldstein and H. Yakowitz (Plenum, New York, 1975), p. 49.

⁷B. D. Hughes and M. F. Shlesinger, *J. Math. Phys.* **23**, 1968 (1982).

⁸R. Rammal and G. Toulouse, *J. Phys. (Paris), Lett.* **44**, L13 (1983).

⁹Y. Gefen *et al.*, *Phys. Rev. Lett.* **47**, 1771 (1981).

¹⁰Y. Gefen *et al.*, *Phys. Rev. Lett.* **50**, 77 (1983).

¹¹P. G. deGennes, *J. Phys. (Paris), Lett.* **87**, L1 (1976).

¹²*Crystal Growth: An Introduction*, edited by P. Hartman (North-Holland, New York, 1973).